Petroleum Science 23 (2026) 5992–6003

Contents lists available at ScienceDirect

Petroleum Science

journal homepage: www.keaipublishing.com/en/journals/petroleum-science

Original Paper

Synergistic effects of carbonated water flooding coupled with surfactant for EOR and CO_2 storage: Pore-scale mechanisms and influencing factors analysis

Xiao-Bing Han [a], Hai-Yang Yu [a,*], Hai-Feng Yang [a], Peng Song [b], Jia-Bang Song [a], Yu-Meng Wang [a], Hui-Ting Tang [a], Yang Wang [a,**]

[a] State Key Laboratory of Petroleum Resources and Engineering, China University of Petroleum (Beijing), Beijing, 102249, China
[b] Research Institute of Exploration and Development, PetroChina Changqing Oilfield Company, Xi'an, 710018, Shaanxi, China

ARTICLE INFO

Article history:
Received 3 September 2025
Received in revised form
16 December 2025
Accepted 20 March 2026
Available online 25 March 2026

Edited by Min Li

Keywords:
Carbonated water
Surfactant
Pore-scale oil displacement characterization
CO_2 storage
Parametric analysis

ABSTRACT

Active carbonated water (ACW) flooding combines the benefits of carbonated water (CW) and surfactant flooding, simultaneously enhancing oil recovery and facilitating CO_2 storage. Nevertheless, the enhanced oil recovery (EOR) mechanisms of ACW remain insufficiently understood, and neither its CO_2 storage performance nor its pore-scale oil displacement characterization have yet to be investigated. Additionally, the influence of different factors on the performance of ACW has not been systematically studied. In this study, core flooding and nuclear magnetic resonance scanning experiments were conducted to elucidate the EOR mechanisms of ACW, clarify for the first time its CO_2 storage performance and pore-scale oil displacement characterization, and examine the influence of various factors on its effectiveness. The results demonstrated that CW flooding enhanced the oil recovery by 12.24% compared to water flooding (46.19%). By leveraging the synergistic effects of CW and surfactant, ACW further increased oil recovery to 64.55%, with pore-scale recovery of 72.22%, 50.77%, and 29.29% for macropores, mesopores, and micropores, respectively, representing increases of 15.77%, 15.05%, and 10.39% relative to water flooding. Furthermore, both CW and ACW demonstrated effective CO_2 storage, with dissolution trapping emerging as a critical mechanism. Compared to the CO_2 storage efficiency of CW at 50.57%, ACW showed a higher efficiency of 52.84%. Within the parameter ranges studied, the oil recovery and CO_2 storage efficiency of ACW both increased with decreasing injection rate and with increasing permeability and surfactant concentration. Correlation analysis revealed that for both metrics, permeability had the most significant influence, followed by surfactant concentration and injection rate. This work provides new insights into the potential of ACW flooding for simultaneous EOR and CO_2 storage, offering practical guidance for its application in low-permeability reservoirs.

1. Introduction

Greenhouse-gas emissions have significantly exacerbated global warming. Among anthropogenic greenhouse gases, CO_2 has a particularly pronounced impact and serves as a major driving force behind this trend (Jeffry et al., 2021; Wang et al., 2023; Li, 2026). Therefore, CO_2 is one of the key mitigation targets in current global emission reduction strategies. Carbon Capture, Utilization, and Storage (CCUS) technology has been proposed as a promising approach to reduce CO_2 emissions and enable large-scale CO_2 sequestration (Lin et al., 2022; Di et al., 2025). Accordingly, various industries have been investigating feasible approaches to CO_2 sequestration (Wang et al., 2025; Xu et al., 2025; Gan et al., 2025; Xie et al., 2026). Oil reservoirs provide a naturally favorable setting for CO_2 sequestration. Enhanced oil recovery (EOR) using CO_2 injection represents a critical strategy within CCUS, as it simultaneously enhances oil recovery and facilitates

* Corresponding author.
** Corresponding author.
E-mail addresses: haiyangyu.cup@139.com (H.-Y. Yu), petroyang@cup.edu.cn (Y. Wang).
Peer review under the responsibility of China University of Petroleum (Beijing).

https://doi.org/10.1016/j.petsci.2026.03.044

CO_2 storage. When CO_2 is injected into the formation and comes into contact with crude oil, it readily dissolves and may become miscible with the oil, thereby reducing oil viscosity, inducing oil swelling, and lowering interfacial tension (IFT). These mechanisms result in enhanced oil displacement efficiency (Wang et al., 2019; Li et al., 2025a; Song et al., 2025). Simultaneously, CO_2 remains trapped within reservoir pores, dissolves in formation water and crude oil, thereby contributing to CO_2 storage and emissions reduction (Han et al., 2024; Kasala et al., 2025; Xiong et al., 2025). However, the significant viscosity and density disparities between CO_2 and crude oil frequently induce viscous fingering and gravity override, consequently compromising sweep efficiency and hindering both oil recovery and CO_2 storage (Luo et al., 2023; Qian et al., 2019; Li et al., 2025b). Consequently, water-alternating-gas and simultaneous water-and-gas injection strategies have been proposed to mitigate challenges associated with adverse mobility ratios and suppress gas override through alternating or concurrent water and gas slug injections (Afzali et al., 2018; Liu et al., 2025). Despite partially mitigating some drawbacks of direct CO_2 flooding, these techniques often induce water shielding, which critically impedes CO_2 transfer to crude oil and weakens oil flow within the formation (Dong et al., 2005; Majidaie et al., 2012).

To mitigate the aforementioned challenges, carbonated water (CW) flooding has emerged as a promising alternative strategy. This approach entails dissolving CO_2 in water and then injecting CW into the reservoir to enhance oil recovery (Han et al., 2025a; Shimokawara et al., 2017; Chen et al., 2026). In contrast to conventional CO_2 flooding, CW exhibits improved sweep efficiency. CW can also improve oil displacement efficiency relative to water flooding (Esene et al., 2019; Talebi et al., 2022). Upon contact with crude oil, dissolved CO_2 progressively migrates to the oil phase, reducing oil viscosity, swelling the oil, improving wettability, and reducing IFT, thereby increasing oil recovery (Han et al., 2024; Seyyedi et al., 2015; Du et al., 2026). Nowrouzi et al. (2020) demonstrated via contact-angle measurements that the core contact angle was reduced to 24.16° after contact with CW, indicating a shift toward a more water-wet state, and wettability improvement exhibited a positive correlation with increasing pressure. Sohrabi et al. (2009, 2011, 2015) performed comprehensive microfluidic investigations of CW flooding; their results showed that the swelling factors of degassed crude oil and *n*-decane increased by 23% and 94%, respectively, following CW injection. Furthermore, the IFT between CW and oil was reduced. Zou et al. (2019) reported findings consistent with those of Sohrabi et al. by conducting core flooding and multiple-contact experiments between CW and oil. After contact with CW, the oil viscosity decreased by approximately 18%, the oil volume increased by approximately 26.0%, and CW flooding improved oil recovery by 20.3% compared with water flooding. To elucidate the mechanism of oil recovery enhancement by CW, researchers have investigated the pore-scale oil displacement characterization during CW flooding. Pan et al. (2024) comparatively analyzed the pore-scale oil displacement characterization of water flooding, surfactant flooding, and CW flooding, and demonstrated that water flooding and surfactant flooding primarily mobilized oil from micropores and macropores, whereas CW flooding could efficiently mobilize oil from nano- and sub-micron pores. Specifically, the oil recoveries for water flooding, surfactant flooding, and CW flooding were 28.9%, 32.6%, and 39.3%, respectively. Xue et al. (2025) reached comparable conclusions, reporting that CW flooding further improved oil recovery to varying extents in both macropores and micropores following water flooding.

Moreover, CW flooding has shown promising CO_2 storage potential. CO_2 dissolution in the CW and oil phases effectively reduces the risk of CO_2 migration. Concurrently, owing to its higher density compared to natural brine, CW settles by gravity to the reservoir bottom, thereby minimizing caprock dependency for secure CO_2 storage and substantially reducing leakage risk (Salehpour et al., 2020; Zhang et al., 2026). Seyyedi et al. (2017) performed core flooding experiments and found that the CO_2 storage efficiency of CW flooding was approximately 42%. Zou et al. (2018) employed gas chromatography to quantify the CO_2 storage efficiency of CW flooding, with a reported efficiency of 39.7%. Bakhshi et al. (2018) examined the effects of salinity, crude oil properties, and injection methods on the CO_2 storage efficiency of CW flooding. They found that low salinity, light oil, and tertiary CW flooding were all favorable for improving CO_2 storage efficiency. Foroozesh and Jamiolahmady (2016, 2018) conducted numerical simulations to investigate CO_2 storage performance of CW flooding at the core scale, finding CO_2 storage efficiencies of 44% for mixed-wet cores and 49% for water-wet cores.

Although CW flooding can enhance oil recovery and enable CO_2 storage, its effectiveness can still be improved. To further enhance its performance, active CW (ACW) flooding has been proposed. This method involves adding a surfactant to CW to form ACW, thereby further improving oil recovery and CO_2 storage (Yu et al., 2019a; Tan et al., 2025; Han et al., 2025b). Alabdulbari et al. (2022) combined low-salinity CW with an ionic liquid-based surfactant to evaluate the effect of the combined system on IFT. The CW and ionic liquid combined system reduced the IFT from 28.70 to 0.98 mN/m. Even under high salinity conditions, adding an ionic liquid-based surfactant to CW can significantly reduce the IFT (Yuan et al., 2023). Yu et al. (2019a, 2019b) conducted core flooding experiments in tight oil reservoirs, showing that ACW flooding following water flooding increased oil recovery by approximately 10% compared with water flooding. Chen et al. (2021) reached similar conclusions, finding that ACW flooding following water flooding had a greater effect on IFT reduction and improved oil recovery by 4% compared to CW flooding following water flooding.

Although existing research has indicated that ACW flooding is a promising EOR technique, current studies have primarily focused on oil recovery improvement. The mechanism by which it enhances oil recovery has not been fully elucidated; the pore-scale oil displacement behavior remains unclear; and the CO_2 storage performance of ACW has not yet been reported in the literature. Furthermore, there is a lack of systematic research on the influence of key factors on the EOR and CO_2 storage performance of ACW flooding. In this study, core flooding and NMR scanning experiments were conducted, revealing for the first time the pore-scale oil displacement characterization and CO_2 storage efficiency of ACW. This study systematically investigated the effects and mechanisms by which CW and ACW enhance oil recovery and CO_2 storage. It also evaluated the influence of surfactant concentration, permeability, and injection rate on the EOR and CO_2 storage efficiency of ACW flooding. Furthermore, grey relational analysis was employed to assess the relationships between key factors and the oil recovery and CO_2 storage efficiency of ACW flooding, offering new insights into the potential of ACW flooding for EOR and CO_2 storage.

2. Research methodology

2.1. Experimental materials

2.1.1. Cores

Outcrop core samples from a nearby location were used in this experimental study. The experimental cores were cylindrical plugs approximately 10 cm in length and 2.5 cm in diameter. These sandstone cores were predominantly composed of quartz, which has limited reactivity with CO_2. Except for those specifically used to investigate the effect of permeability, the cores employed for comparison experiments exhibited similar petrophysical properties, with an average porosity of 16.07% and an average permeability of 15.09 mD, to ensure experimental comparability. The petrophysical parameters of the experimental cores are summarized in Table 1.

2.1.2. Oil

The experimental oil was a recombined live oil sample. As presented in Table 2, at the reservoir temperature (72 °C) and pressure (25 MPa), the oil exhibited a density of 0.709 g/cm^3 and a viscosity of 0.494 mPa·s, indicating that the oil was low-viscosity. Based on the carbon number distribution, the crude oil was divided into light components ($\leq C_{17}$) and heavy components ($>C_{17}$), with corresponding molar fractions of 86.89% and 12.12%, respectively, while the remaining components consisted of CO_2 and N_2.

2.1.3. Surfactant

The surfactant used in the experiments was obtained from the target field. It is a zwitterionic surfactant characterized by exceptional salt tolerance and a wide range of applicability. The critical micelle concentration of the surfactant was 0.03 w.t.%, whereas the field-applied concentration was 0.10 w.t.% to compensate for potential surfactant loss. This concentration was maintained throughout the experimental series except in targeted experiments designed to investigate the effect of surfactant concentration. To suppress hydrogen signals during NMR and enable pore-scale oil-displacement characterization, a 12.0 w.t.% manganese chloride solution was prepared as the experimental water. CO_2 and the surfactant were dissolved in the manganese chloride solution for subsequent experiments. Using the spinning drop method at reservoir temperature and atmospheric pressure, IFT measurements showed that the surfactant solution prepared with the same base fluid and at the field concentration reduced the degassed reservoir oil–water IFT to approximately 1×10^{-2} mN/m. Separately, contact angle measurements conducted at 25 °C and atmospheric pressure using the sessile-drop method showed that exposure to the surfactant solution substantially altered the core wettability, decreasing the oil–water–rock contact angle from 120° to 65°.

Table 1
Core physical properties.

Core	Length, cm	Diameter, cm	Permeability, mD	Porosity, %
A-1	10.031	2.501	14.94	16.24
A-2	10.066	2.508	15.28	16.00
A-3	10.029	2.507	15.15	16.17
A-4	10.056	2.498	15.20	15.88
A-5	10.026	2.505	15.36	16.25
A-6	10.033	2.502	14.67	16.02
A-7	10.012	2.511	15.02	15.96
A-8	10.041	2.503	5.01	10.68
A-9	10.052	2.499	24.89	18.24

Table 2
Crude oil properties.

Property	Density, g/cm^3	Viscosity, mPa·s	Saturation pressure, MPa	Light component molar fraction, %	Heavy component molar fraction, %
Value	0.709	0.494	9.532	86.89	12.12

2.1.4. Carbonated water

The concentration of CW employed in all experiments was 1.0 mmol/cm^3. The amount of CO_2 was calculated based on the predetermined volume and concentration of the CW. At the target temperature, accounting for the compressibility of CO_2, the calculated amount of gas was injected into a stirred intermediate vessel. Water was subsequently added until the target pressure was reached, and stirring was maintained to facilitate CO_2 dissolution. During this process, CO_2 dissolution led to a pressure decline, and additional water was injected intermittently to restore the pressure until a stable pressure was achieved. To ensure complete CO_2 dissolution, stirring was continued for an additional 24 h. ACW is CW with added surfactant, which synergistically integrates the advantageous properties of both CW and surfactant. ACW was prepared by dissolving CO_2 in the surfactant solution. Regardless of whether CW or ACW was prepared, after completion of the procedure, a portion of the fluid was discharged at a low flow rate through a constant-rate or constant-pressure pump coupled with a back-pressure regulator. The gas-to-water ratio of the discharged stream was continuously monitored to verify complete CO_2 dissolution and attainment of the target concentration.

2.2. Experimental setup and procedures

Comprehensive core flooding and NMR scanning experiments were conducted to elucidate the mechanisms of oil displacement and CO_2 storage of ACW, characterize pore-scale oil displacement, and evaluate the impact of key factors on ACW effectiveness. Fig. 1 presents a schematic diagram of the experimental setup, comprising a constant-rate or constant-pressure pump, an intermediate vessel, an NMR scanning device, a gas flow meter, and a gas chromatograph. By collecting, measuring, and analyzing the effluent fluids, oil recovery and CO_2 storage efficiency were quantified. NMR scanning was employed to assess oil recovery within pores of different size ranges.

NMR scanning provides the T_2 spectrum of the experimental core, which offers a visual representation of the transverse relaxation time distribution, and enables comprehensive characterization of pore structure and fluid content. The T_2 relaxation time is composed of surface relaxation time ($T_{2,\text{surface}}$), bulk relaxation time ($T_{2,\text{bulk}}$), and diffusion relaxation time ($T_{2,\text{diffusion}}$), as shown in Eq. (1) (Tang et al., 2022; Zhang et al., 2021):

$$\frac{1}{T_2} = \frac{1}{T_{2,\text{bulk}}} + \frac{1}{T_{2,\text{surface}}} + \frac{1}{T_{2,\text{diffusion}}} \tag{1}$$

In porous media, the bulk relaxation time is typically long enough to be neglected, and because the internal magnetic field of the instrument is sufficiently homogeneous, the diffusion relaxation time can likewise be disregarded. T_2 primarily depends on surface relaxation and can be expressed as shown in Eq. (2):

$$T_2 = T_{2,\text{surface}} = \frac{V}{\rho_t S} \tag{2}$$

where, S is pore surface area, μm^2; V is pore volume, μm^3; ρ_t is the surface relaxivity, μm/ms.

For porous media, the relationship between S and V can be expressed as shown in Eq. (3):

$$\frac{S}{V} = \frac{F_s}{r} \tag{3}$$

where, F_s is the pore shape factor; r is the pore radius, μm.

By combining Eq. (2) and Eq. (3), Eq. (4) can be obtained as follows:

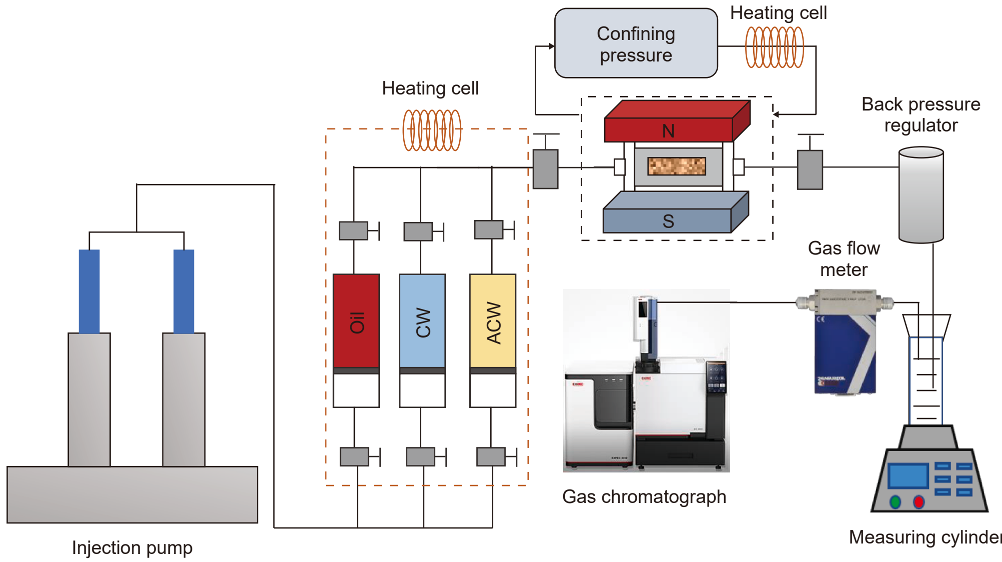

Fig. 1. Schematic illustration of the experimental apparatus.

$$T_2 = \frac{r}{\rho_t F_s} \tag{4}$$

Therefore, T_2 is proportional to pore radius. It should be noted that Eq. (4) neglects both the bulk and diffusion relaxation times. In addition, this equation represents a simplified model that idealizes the actual pore structure as a system of spherical or cylindrical pores and throats. Despite these simplifications, the equation establishes a quantitative relationship between T_2 and pore radius and thus serves as a useful approximation. Based on the T_2 values, the pores are classified into micropores (<10 ms), mesopores (10–100 ms), and macropores (>100 ms) (An et al., 2022). The T_2 signal intensity serves as a quantitative indicator of fluid content within the core pores. Oil recovery is determined by analyzing the changes in the T_2 spectrum area (Eq. (5)):

$$Recovery = \frac{S_{\text{initial}} - S_{\text{residual}}}{S_{\text{initial}}} \times 100\% \tag{5}$$

where, S_{initial} is the T_2 spectrum area of the core saturated with oil; S_{residual} is the T_2 spectrum area of the core after displacement.

The specific experimental steps are as follows.

(1) The core sample was evacuated under vacuum for 24 h, then saturated with distilled water under pressure for 72 h.
(2) The experimental apparatus was assembled, and the test temperature was maintained at 72 °C. The confining pressure was set to track the inlet pressure and was kept 3 MPa higher throughout the experiment, while the outlet back-pressure was held constant at 25 MPa.
(3) The core was flooded with a manganese chloride solution to ensure full saturation. Subsequently, an NMR scan was conducted to confirm suppression of the hydrogen signal.
(4) Oil injection was performed to displace water until no water was observed in the effluent, establishing irreducible water saturation. Following core sample aging, a subsequent NMR scan was performed.
(5) The displacing fluid was injected into the core at a constant rate of 0.1 cm^3/min. The displaced fluids were collected and analyzed. An NMR scan was performed until 1.2 PV was injected.
(6) The experimental core was replaced with a new one, and the displacing fluid and injection rate were appropriately adjusted in accordance with the research objective. Steps (1) to (5) were systematically repeated.

3. Results and discussion

3.1. Mechanisms of ACW for EOR and CO_2 storage

3.1.1. Enhanced oil recovery

Water flooding, CW flooding, and ACW flooding experiments were conducted using cores A-1 through A-3, respectively. Fig. 2 illustrates the oil recovery curves as a function of injected fluid volume for the various displacement methods. All recovery curves show a rapid increase in oil recovery at early injected volumes,

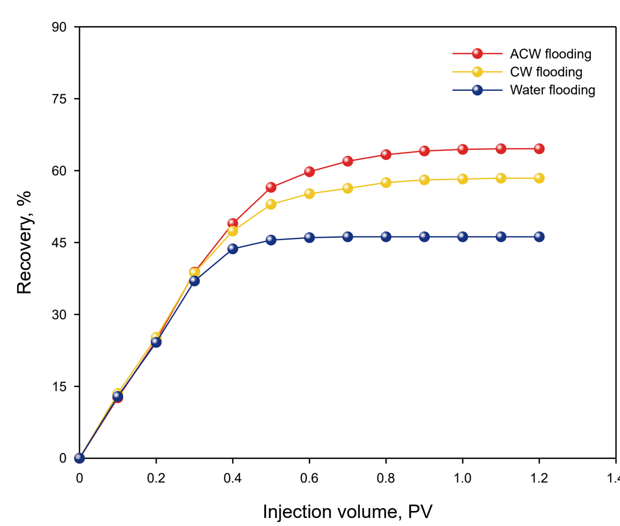

Fig. 2. Oil recovery variation with injection volume under different displacement methods.

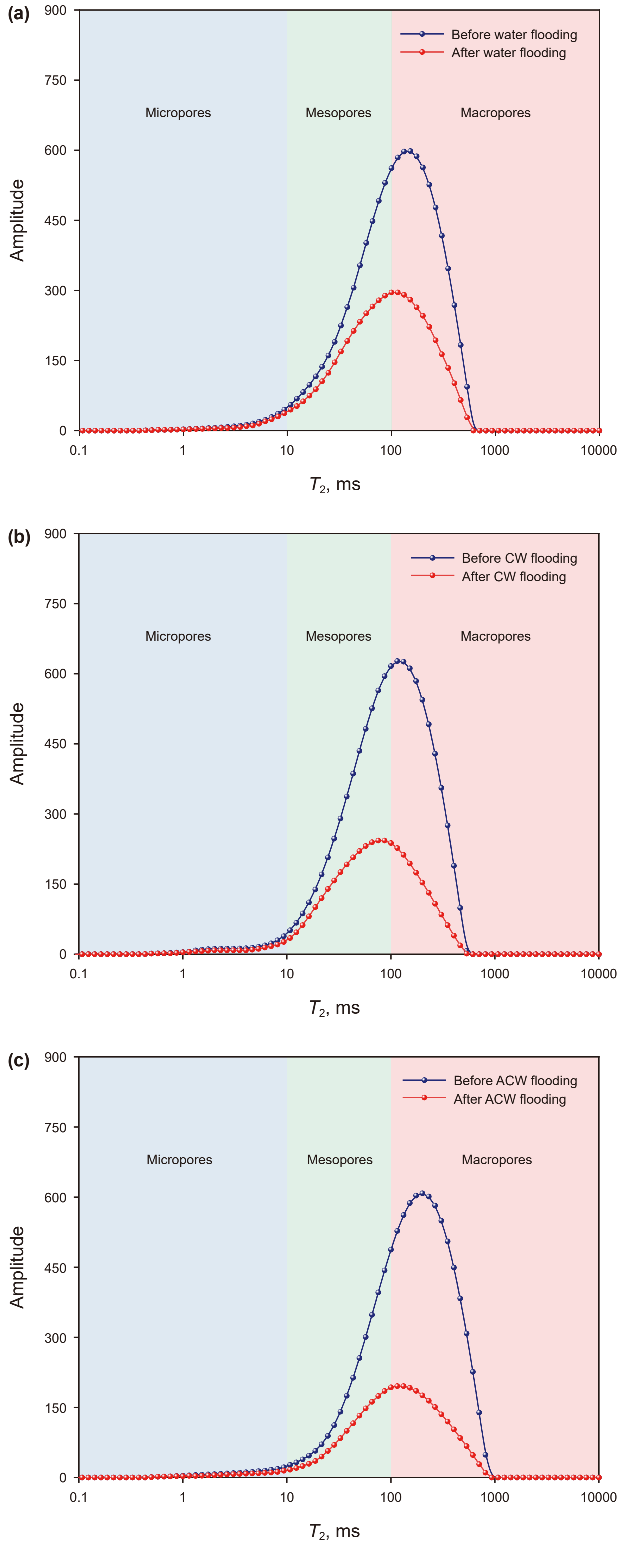

Fig. 3. Comparison of T_2 spectra before and after displacement by different methods. **(a)** Water flooding; **(b)** CW flooding; **(c)** ACW flooding.

followed by a gradual increase at later stages. Compared to water flooding, CW and ACW flooding achieved oil recovery improvements of 12.24% and 18.36%, respectively, indicating improved displacement efficiency.

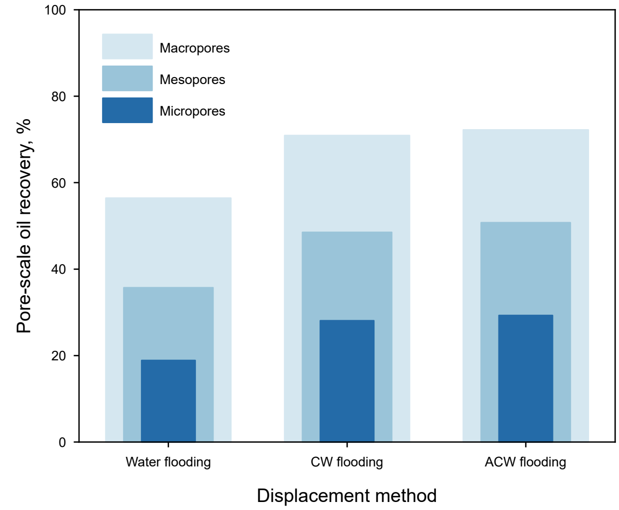

Fig. 4. Comparison of pore-scale oil recovery under various displacement methods.

Fig. 3 depicts the T_2 spectral variations in the core samples before and after fluid displacement. The magnitude of spectral changes is generally associated with oil recovery. Fig. 4 presents the pore-scale oil recovery, quantified through T_2 spectral analysis. Both CW and ACW flooding demonstrated higher recovery across macropores, mesopores, and micropores compared to conventional water flooding. Owing to the inherent low permeability of the reservoir and the limited oil displacement capabilities of water, conventional water flooding yielded an oil recovery of 46.19%. Water flooding predominantly mobilized oil from macropores, with limited oil mobilization from micropores. The recoveries for macropores, mesopores, and micropores were 56.45%, 35.72%, and 18.90%, respectively. In contrast to conventional water flooding, CW flooding substantially enhanced overall oil recovery to 58.43%, with oil recovery from macropores, mesopores, and micropores of 70.93%, 48.54%, and 28.09%, respectively. Fig. 5 illustrates the EOR mechanisms of CW. The dissolved CO_2 in CW interacts with oil, progressively migrating from the aqueous phase into the oil phase, thereby swelling the oil and reducing its viscosity. Concurrently, CO_2 dissolution forms carbonic acid, reducing the aqueous phase pH. This enables CW to modify the surface charge at the oil/water/rock interfaces and facilitate reactions with the rock mineral surfaces, consequently improving wettability (Sohrabi et al., 2015). Fig. 6 shows contact-angle changes before and after CW flooding. After CW flooding, the contact angle decreased from 117.7° to 94.9°. Moreover, CW interacts with the light components in oil, and CO_2 migration from the aqueous phase to the oil-water interface weakens hydrogen bonding among water molecules, consequently reducing the IFT to a single-digit range (Rahimi et al., 2020; Chen et al., 2024).

By combining CW with a surfactant, ACW achieved an overall oil recovery of 64.55%. Compared to water flooding, oil recovery from macropores, mesopores, and micropores increased by 15.77%, 15.05%, and 10.39%, respectively. The primary mechanisms by which ACW enhances oil recovery are as follows: (1) The surfactant improved wettability and reduced IFT. ACW reduced the IFT to a level of 0.01 mN/m, and the contact angle decreased from 120.9° to 53.2° after ACW flooding (Fig. 7), thereby facilitating ACW penetration into smaller pores. This mechanism enables more efficient CO_2 mass transfer, contributing to enhanced oil displacement efficiency. (2) The acidic environment generated by CW may protonate the zwitterionic surfactant, promoting surfactant adsorption at the oil-water interface and on the rock surface.

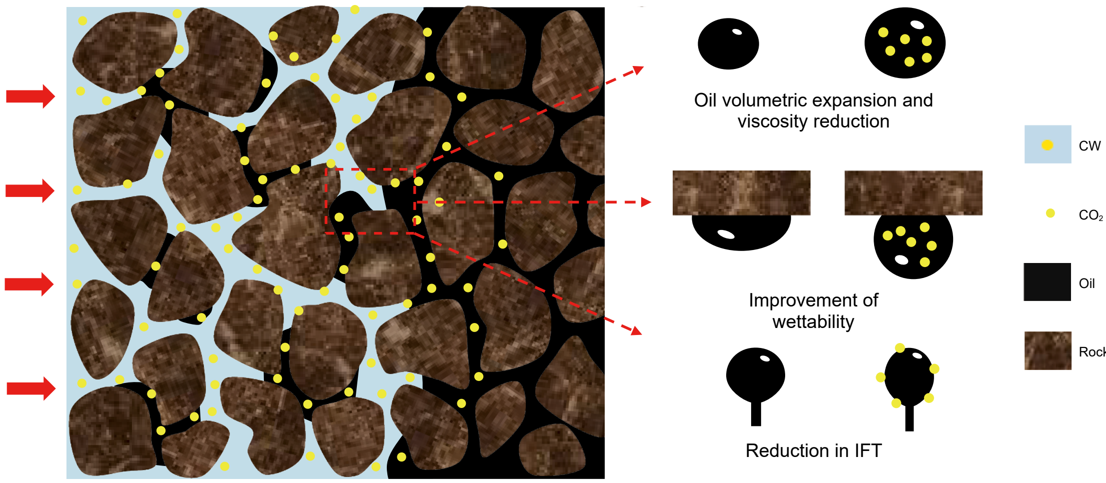

Fig. 5. Schematic diagram of the mechanism of EOR by CW flooding.

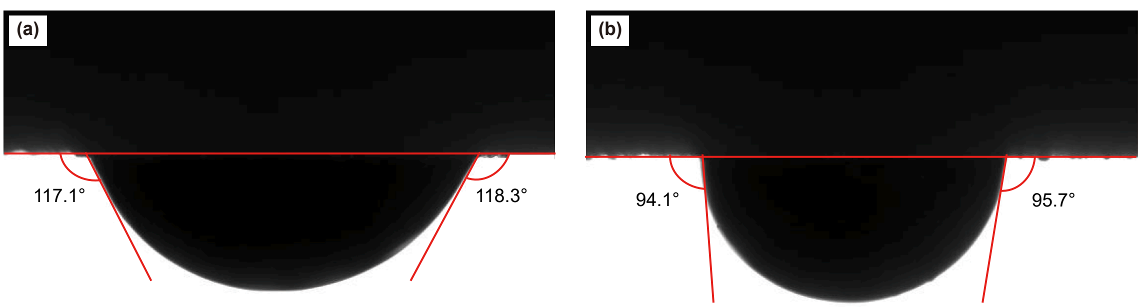

Fig. 6. Comparison of contact angles. **(a)** Before CW flooding; **(b)** After CW flooding.

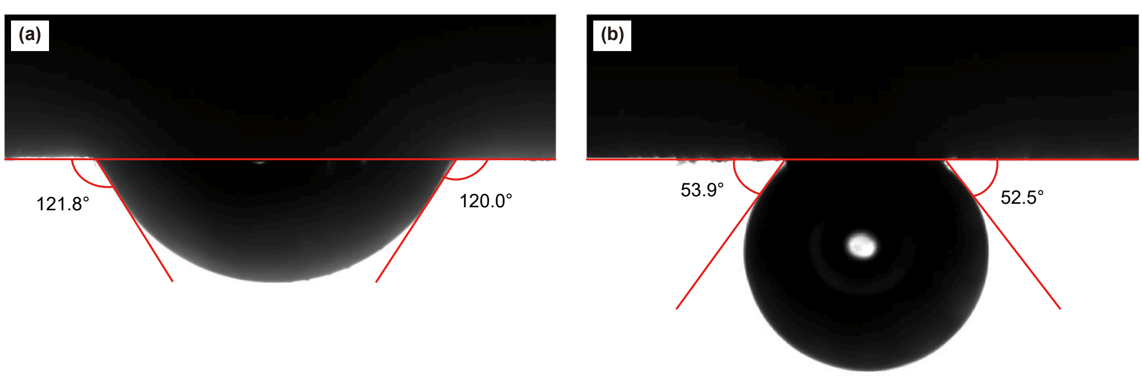

Fig. 7. Comparison of contact angles. **(a)** Before ACW flooding; **(b)** After ACW flooding.

This forms a more stable and denser adsorption layer, which improves wettability and reduces IFT (Al-Sadat et al., 2014; Wu et al., 2022; Sun et al., 2024).

Fig. 8 presents a comparison of NMR imaging results obtained before and after displacement using different fluids. Hydrogen signal intensity serves as a quantitative proxy for oil content, with higher values indicating greater oil saturation. The magnitude of hydrogen signal intensity changes tends to correlate with oil recovery. ACW flooding exhibited the most pronounced hydrogen signal intensity variations, corresponding to the highest oil recovery, followed by CW flooding and water flooding. These findings align well with the core flooding and NMR T_2 spectral analysis results, supporting the consistency of the experimental data. Throughout the displacement process, the pressure at the inlet end remained higher than that at the outlet end. The oil distribution within the core after the experiment indicated lower oil saturation at the inlet end (left side) and higher oil saturation at the outlet end (right side). Furthermore, compared to water flooding, the difference in oil saturation between the left and right sides was more pronounced for CW and ACW flooding. The results suggest that: (1) Elevated pressure leads to enhanced oil displacement efficiency, while simultaneously increasing difference in CO_2 solubility between oil and water phases. These phenomena influence oil recovery and consequently result in a more pronounced

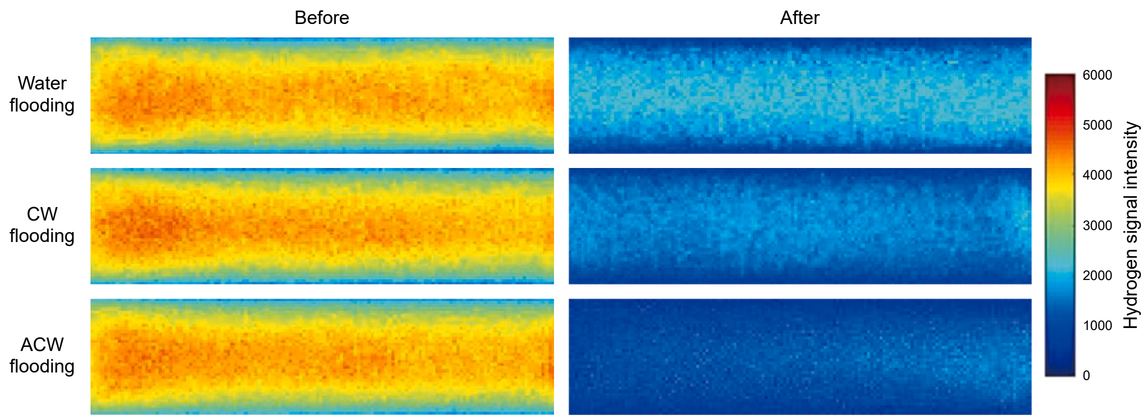

Fig. 8. Comparison of NMR imaging results before and after displacement by different methods.

inlet–outlet saturation gradient across the core during CW and ACW flooding. (2) Compared with the outlet end, the inlet end had a longer contact time with CW and ACW, allowing the effects of CO_2 and the surfactant to be more effectively realized. Consequently, formation pressure exerts a more pronounced influence on CW and ACW flooding compared to conventional water flooding. Increasing formation pressure and enhancing CW or ACW-oil contact can improve oil recovery.

3.1.2. *CO_2 storage efficiency*

In contrast to CO_2 flooding, CO_2 remains in a dissolved state within CW, mitigating CO_2 mobility in reservoir formations and minimizing leakage risk. For a given CO_2 concentration in CW/ACW and a fixed injection volume, the total amount of injected CO_2 was calculated accordingly. By collecting the produced gas at the outlet and quantifying the produced CO_2 through chromatographic analysis after the experiment, the CO_2 storage efficiency was determined by comparing the difference between the injected and produced CO_2 with the total amount injected (Hao et al., 2022). Fig. 9 compares CO_2 storage efficiency for the different displacing fluids. CW and ACW demonstrated CO_2 storage efficiencies of 50.57% and 52.84%, respectively. These results support the potential for effective CO_2 sequestration, with ACW exhibiting slightly higher storage performance.

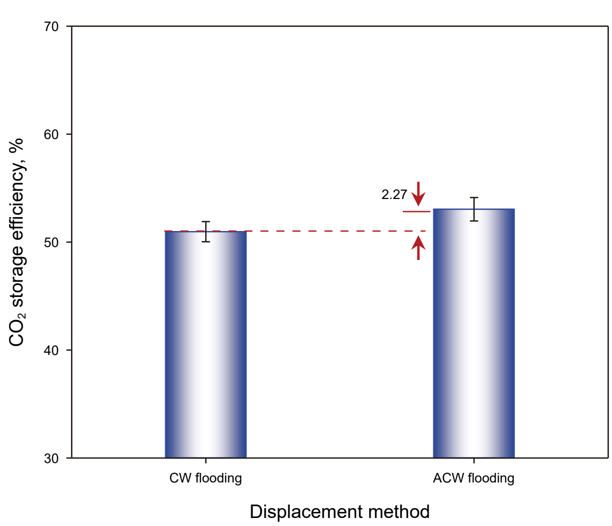

Fig. 9. Comparison of CO_2 storage efficiency between CW and ACW flooding.

Given the experimental constraints of short-duration core flooding and the core's predominantly quartz mineralogical composition, the interactions between CO_2 and the rock matrix via mineralization were considered negligible (Berndsen et al., 2024; Seyyedi and Sohrabi, 2016). Consequently, dissolution trapping emerged as the predominant CO_2 storage mechanism in CW and ACW flooding experiments. As flooding proceeds, the injected fluid progressively occupies pore space within the core. A fraction of CO_2 dissolves in CW, with additional CO_2 partitioning into the residual oil and irreducible water (Salehpour et al., 2020; Sohrabi et al., 2011; Dang et al., 2025). In contrast to CW flooding, ACW flooding resulted in higher oil recovery, thereby reducing the residual oil volume, which limited the capacity for CO_2 dissolution in the residual oil. However, CO_2 storage efficiency was still higher for ACW than for CW flooding. The primary mechanisms for this are: (1) ACW could penetrate smaller core pores, enabling more comprehensive interaction with residual oil, thus enhancing CO_2 dissolution per unit residual oil volume. (2) The delayed breakthrough behavior of ACW flooding enabled prolonged oil displacement and increased pore space occupancy, thereby improving CO_2 storage efficiency.

3.2. *Investigation of factors influencing recovery and CO_2 storage efficiency*

3.2.1. *Surfactant concentration*

ACW flooding experiments were performed on cores A-4 (0.05 w.t.%) and A-5 (0.20 w.t.%), respectively. Together with the experimental results for core A-3, the influence of surfactant concentration on ACW flooding performance was evaluated. As depicted in Fig. 10, increasing surfactant concentration generally increased the oil recovery. Specifically, raising the surfactant concentration from 0.05 w.t.% to 0.10 w.t.% led to an increase in oil recovery from 60.82% to 64.55%. However, further increasing the concentration to 0.20 w.t.% yielded a marginal oil recovery improvement of merely 1.87%. Throughout the displacement process, the surfactant adsorbed onto pore surfaces and the oil-water interface, effectively improving wettability and reducing IFT. This reduces oil flow resistance and enables ACW penetration into smaller core pores, thereby promoting CO_2 diffusion into oil and enhancing oil mobility. Increasing surfactant concentration promotes the full realization of its potential. However, upon exceeding the critical micelle concentration, surfactant efficacy tends to reach a performance plateau, resulting in only marginal improvements in oil recovery.

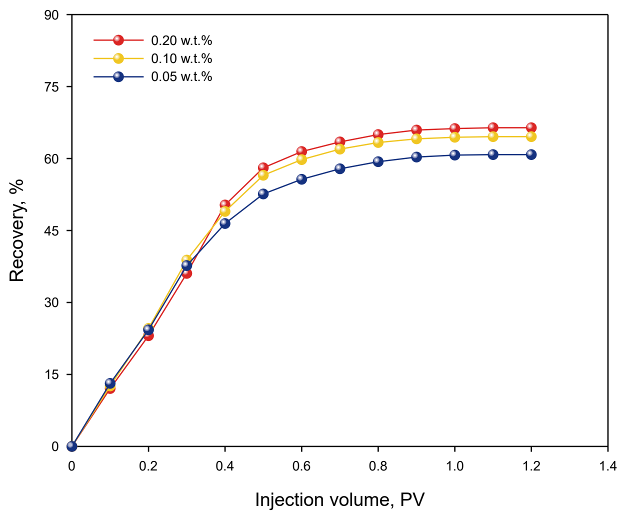

Fig. 10. Variation of oil recovery with injection volume for ACW flooding at different surfactant concentrations.

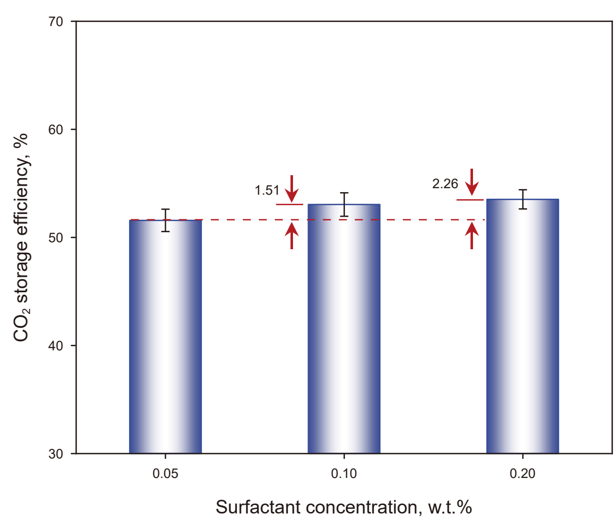

Fig. 11. Comparison of CO_2 storage efficiency for ACW flooding at different surfactant concentrations.

Fig. 11 compares CO_2 storage efficiency at different surfactant concentrations. Increasing the surfactant concentration enhances the contact between ACW and oil, thereby facilitating CO_2 diffusion into the oil and improving CO_2 storage efficiency. Consistent with the oil recovery trend, the incremental gain in CO_2 storage efficiency diminished as surfactant concentration increased. At a surfactant concentration of 0.05 w.t.%, ACW flooding demonstrated a CO_2 storage efficiency of 51.33%. Increasing the surfactant concentration to 0.10 w.t.% and 0.20 w.t.% yielded CO_2 storage efficiency improvements of 1.51% and 2.26%, respectively. Given that surfactants are costly EOR agents, selecting an optimal surfactant concentration is a key factor in achieving efficient incremental oil recovery and improved economic viability. Moreover, surfactant performance is a critical determinant of ACW flooding efficacy. In addition to effectively improving wettability and reducing IFT, an optimal surfactant capable of enhancing CO_2 dissolution in water could further enhance the effectiveness of ACW flooding.

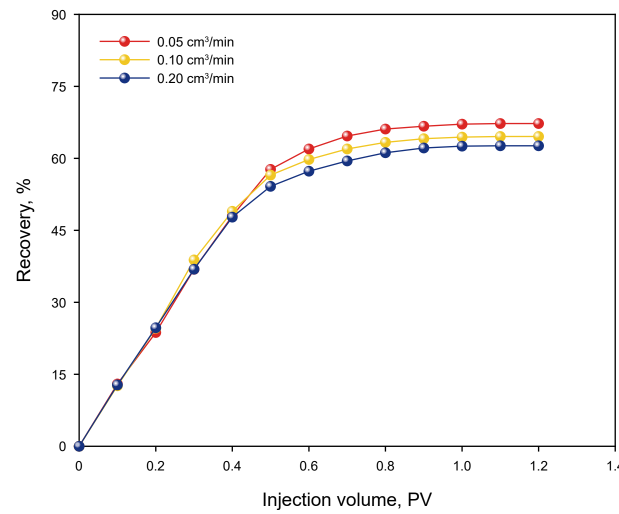

Fig. 12. Variation of oil recovery with injection volume for ACW flooding at different injection rates.

3.2.2. Injection rate

ACW flooding was conducted on cores A-6 and A-7, employing injection rates of 0.05 cm^3/min and 0.20 cm^3/min, respectively. In combination with the experimental results for core A-3, the effect of injection rate on ACW oil displacement efficiency and CO_2 storage performance was analyzed. Fig. 12 illustrates the correlation between oil recovery and injected volume under different injection rates for ACW flooding. Higher injection rates tend to reduce the EOR effectiveness of ACW. At an injection rate of 0.05 cm^3/min, oil recovery improved by 2.71% and 4.64% compared to injection rates of 0.10 and 0.20 cm^3/min, respectively. Lower injection rates promote a more stable displacement front, facilitating better interaction between ACW, oil, and rock surfaces. This enables effective wettability alteration, reduces IFT, induces oil swelling, and lowers viscosity, thereby increasing oil displacement efficiency and sweep efficiency, and ultimately increasing oil recovery.

Fig. 13 compares CO_2 storage efficiency at different injection rates. Reduced injection rates generally correlate with higher CO_2

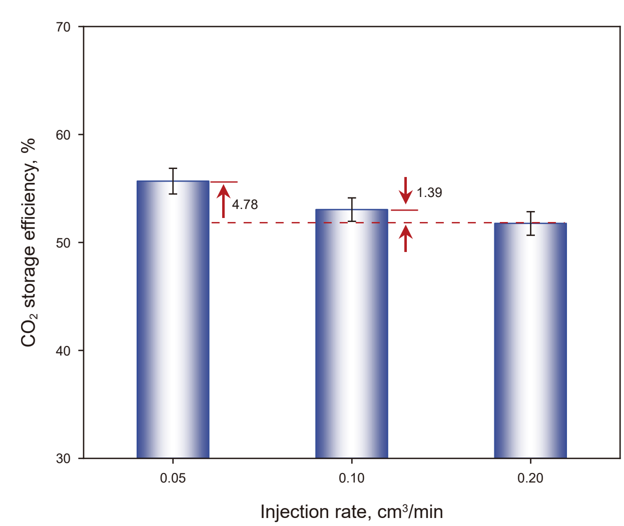

Fig. 13. Comparison of CO_2 storage efficiency for ACW flooding at different injection rates.

storage efficiency. As the injection rate increased from 0.05 cm^3/min to 0.20 cm^3/min, the CO_2 storage efficiency declined from 56.23% to 51.45%. Under high injection rates, elevated fluid flow velocity within the core substantially reduces CO_2 residence time. Conversely, lower injection rates facilitate more extensive CO_2 diffusion into reservoir fluids. Moreover, reduced injection rates correlate with higher oil recovery, increasing the pore volume available for CO_2 occupancy. Therefore, provided that field production requirements are met, a moderate reduction in injection rate may be beneficial for improving oil recovery and enhancing CO_2 storage during ACW flooding.

3.2.3. Permeability

A comparative analysis of cores A-3, A-8, and A-9 was conducted to evaluate the effect of permeability on ACW oil displacement efficiency and CO_2 storage performance. Fig. 14 depicts the relationship between oil recovery and injected volume for ACW flooding across cores with varying permeability. Core permeability correlated positively with oil recovery during ACW flooding. Lower-permeability cores typically have narrow pore throats, leading to increased fluid flow resistance, which in turn hampers displacement efficiency. Moreover, the intricate pore structure and limited pore connectivity in lower-permeability cores impede CO_2 diffusion into crude oil, limiting ACW contact with oil and rock surfaces. This substantially diminishes the overall ACW sweep efficiency. Conversely, higher-permeability cores feature larger pore throat diameters and improved pore connectivity, creating optimal conditions for ACW flooding and consequently resulting in higher oil recovery. Compared to the baseline core with a permeability of 5.01 mD, oil recovery increased by 4.69% and 7.58% for cores with permeability of 15.15 and 24.89 mD, respectively.

Fig. 15 compares CO_2 storage efficiency for cores with different permeabilities of ACW flooding. The experimental data indicate that CO_2 storage efficiency correlated positively with core permeability. As permeability increased from 5.01 to 24.89 mD, CO_2 storage efficiency improved from 48.20% to 56.53%. Higher-permeability cores have larger pore throat diameters and reduced tortuosity, enhancing ACW–oil contact and facilitating more connected pathways for CO_2 diffusion into crude oil. Moreover, higher-permeability cores characteristically exhibit more extensive pore volumes, which are more favorable for CO_2 storage.

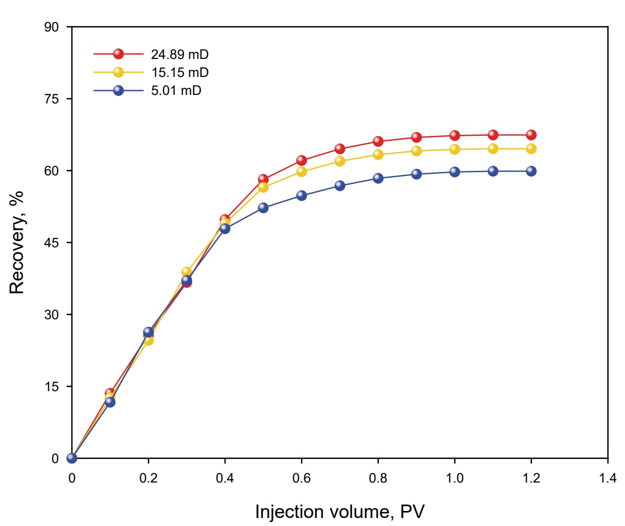

Fig. 14. Variation of oil recovery with injection volume for ACW flooding at different permeability.

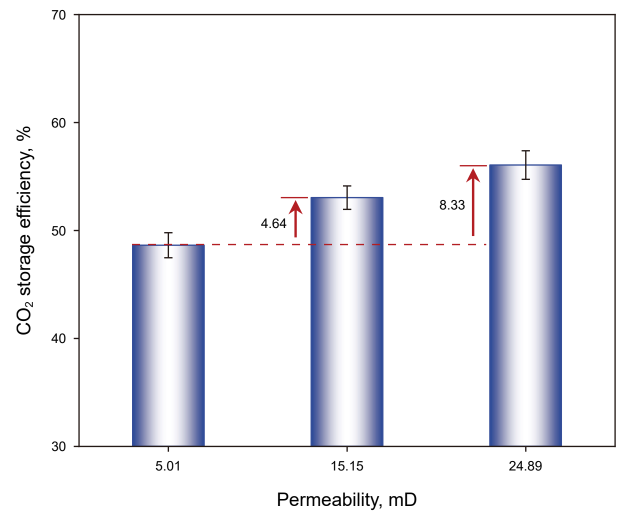

Fig. 15. Comparison of CO_2 storage efficiency for ACW flooding at different permeability.

Consequently, enhancing the flow capacity of low-permeability reservoirs through treatments similar to hydraulic fracturing could further improve the effectiveness of ACW flooding.

3.2.4. Correlation analysis

To elucidate the effects of key factors on ACW flooding, a comprehensive correlation analysis was conducted, examining oil recovery and CO_2 storage efficiency with respect to surfactant concentration, permeability, and injection rate. Given the characteristics of the experimental dataset and the suitability of various analytical approaches, grey relational analysis was selected to assess correlations. Grey relational analysis represents a robust analysis method particularly advantageous for small-sample scenarios, characterized by its independence from distributional assumptions. This approach enables a quantitative assessment of associations, facilitating comprehensive comparative insights (Deng, 1989).

Fig. 16 presents the correlation analysis results. Within the investigated parameter ranges, although the relational grades between the factors and oil recovery and CO_2 storage efficiency varied, the ranking remained consistent. Permeability emerges as a critical determinant of reservoir fluid flow capacity, influencing

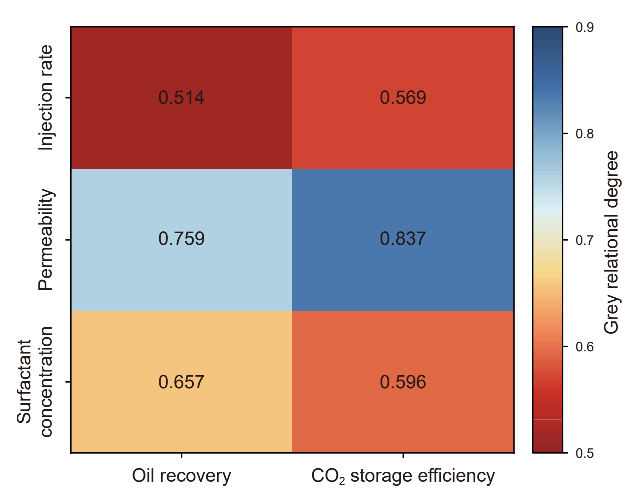

Fig. 16. Results of grey relational analysis.

the contact between ACW and oil, exerting the strongest influence on oil recovery and CO_2 storage efficiency. Surfactant concentration influences oil recovery and CO_2 storage efficiency by improving wettability and reducing IFT, exhibiting a secondary yet significant influence. Injection rate affects the contact time between ACW and oil as well as displacement front stability, with a weaker association with oil recovery and CO_2 storage efficiency compared to permeability and surfactant concentration. Consequently, in low-permeability reservoirs, increasing permeability may be a key approach to enhancing the effectiveness of ACW and have a greater effect than adjusting surfactant concentration or injection rate within the tested ranges. Nevertheless, selecting appropriate surfactant concentration and injection rate remains important for improving ACW performance.

4. Conclusions

CW flooding is an effective EOR method that can simultaneously enhance oil recovery and enable CO_2 storage, whereas ACW flooding can further improve these effects. In this study, core flooding and NMR experiments were conducted to quantify, for the first time, the pore-scale displacement characterization and CO_2 storage efficiency of ACW flooding. This research systematically investigated the effects and mechanisms by which ACW enhances oil recovery and CO_2 storage, clarified the influence of various parameters on ACW performance, and ranked the relative associations between different factors and the oil recovery and CO_2 storage efficiency. This work demonstrates the potential of ACW flooding for EOR and CO_2 storage, offering valuable insights for its application.

(1) CW can induce oil swelling and viscosity reduction, simultaneously improve wettability and reduce IFT. Oil recovery via CW flooding reached 58.43%, representing a 12.24% improvement compared to conventional water flooding. ACW synergistically integrates the benefits of CW and surfactants, substantially improving wettability and reducing IFT, while facilitating CO_2 transfer into the oil phase. Consequently, oil recovery was further increased to 64.55%. The oil recoveries for macropores, mesopores, and micropores were 72.22%, 50.77%, and 29.29%, respectively, which are 15.77%, 15.05%, and 10.39% higher than those of water flooding.

(2) Dissolution trapping represents a critical mechanism for CO_2 sequestration in both CW and ACW flooding. CO_2 predominantly dissolves in water and oil, effectively reducing its mobility and mitigating leakage risk. Both CW and ACW exhibited CO_2 storage capacity. The CO_2 storage efficiency of CW flooding was 50.57%. In comparison, ACW further improved wettability and reduced IFT, increasing the contact between ACW and crude oil, thereby facilitating CO_2 mass transfer. The CO_2 storage efficiency increased to 52.84%.

(3) Within the investigated parameter ranges, a lower injection rate is beneficial for the interaction between ACW, crude oil, and reservoir rock. Decreasing the injection rate from 0.20 to 0.05 cm^3/min resulted in improvements of 4.64% in oil recovery and 4.78% in CO_2 storage efficiency. Higher permeability facilitates fluid flow and improves ACW performance. Compared with 5.01 mD, the oil recovery and CO_2 storage efficiency at 24.89 mD increased by 7.58% and 8.33%, respectively. When the surfactant concentration exceeds approximately 0.10 w.t.%, the rate of increase in oil recovery and CO_2 storage efficiency diminishes significantly. Permeability showed the strongest association, followed by surfactant concentration and injection rate.

This study elucidated the pore-scale oil displacement characteristics and CO_2 storage performance of ACW, and clarified the impacts of various factors on its enhanced oil recovery and CO_2 sequestration effectiveness. However, the mass transfer dynamics of CO_2 from CW and ACW into crude oil were not further investigated. Future studies may focus on this aspect to gain deeper insight into the mechanisms and effectiveness of ACW in mitigating the water-shielding effect. In addition, the favorable oil displacement and CO_2 storage performance of ACW stem from the synergistic advantages of CW and surfactants. The development of surfactants capable of enhancing CO_2 solubility in water, together with the effective utilization of the acidity of CW to further promote surfactant performance in improving wettability and reducing IFT, is expected to further strengthen the synergistic performance of ACW.

CRediT authorship contribution statement

Xiao-Bing Han: Writing – original draft, Methodology, Investigation. **Hai-Yang Yu:** Writing – review & editing, Investigation, Funding acquisition, Conceptualization. **Hai-Feng Yang:** Visualization, Methodology, Formal analysis. **Peng Song:** Validation, Resources, Investigation. **Jia-Bang Song:** Visualization, Validation, Methodology. **Yu-Meng Wang:** Visualization, Methodology. **Hui-Ting Tang:** Methodology, Investigation. **Yang Wang:** Writing – review & editing, Investigation.

Declaration of competing interest

The authors declare that they have no known competing financial interests or personal relationships that could have appeared to influence the work reported in this paper.

Acknowledgement

This work was financially supported by the National Science and Technology Major Project (2025ZD1406204) and the National Natural Science Foundation of China (52074317).

References

Afzali, S., Rezaei, N., Zendehboudi, S., 2018. A comprehensive review on enhanced oil recovery by water alternating gas (WAG) injection. Fuel 227, 218–246. https://doi.org/10.1016/j.fuel.2018.04.015.

Al-Sadat, W., Nasser, M.S., Chang, F., et al., 2014. Laboratory evaluation of the effects of additives and pH on the thermorheological behavior of a viscoelastic zwitterionic surfactant used in acid stimulation. J. Petrol. Sci. Eng. 122, 458–467. https://doi.org/10.1016/j.petrol.2014.08.006.

Alabdulbari, O.A.A., Alabid, F.S.R., Hosseini, S., 2022. Effects of formation brine, [C_{12}mim] [Cl] concentration, temperature and pressure on the swelling factor and IFT of the carbonated water/heavy crude oil system. Braz. J. Chem. Eng. 39 (1), 289–300. https://doi.org/10.1007/s43153-021-00210-6.

An, Q.Y., Zhang, Q.S., Li, X.H., et al., 2022. Static and dynamic alteration effect of SC-CO_2 on rock pore evolution under different temperature and pressure: a comparative study. J. Nat. Gas Sci. Eng. 107, 104780. https://doi.org/10.1016/j.jngse.2022.104780.

Bakhshi, P., Kharrat, R., Hashemi, A., et al., 2018. Experimental evaluation of carbonated waterflooding: a practical process for enhanced oil recovery and geological CO_2 storage. Greenh. Gases: Sci. Technol. 8 (2), 238–256. https://doi.org/10.1002/ghg.1734.

Berndsen, M., Erol, S., Akın, T., et al., 2024. Experimental study and kinetic modeling of high temperature and pressure CO_2 mineralization. Int. J. Greenh. Gas Control 132, 104044. https://doi.org/10.1016/j.ijggc.2023.104044.

Chen, K., Geng, W.Y., Zhang, J.R., et al., 2026. Carbonated water injection as an emerging hybrid enhanced oil recovery technique: a review. Geoenergy Sci. Eng. 257, 214250. https://doi.org/10.1016/j.geoen.2025.214250.

Chen, K., Zhang, J.R., Xu, S.Y., et al., 2024. Review of carbonated water injection as a promising technology to enhance oil recovery in the petroleum industry:

challenges and prospects. Pet. Sci. 21, 4100–4118. https://doi.org/10.1016/j.petsci.2024.07.009.
Chen, X.X., Paprouschi, A., Elveny, M., et al., 2021. A laboratory approach to enhance oil recovery factor in a low permeable reservoir by active carbonated water injection. Energy Rep. 7, 3149–3155. https://doi.org/10.1016/j.egyr.2021.05.043.
Dang, F.Q., Li, S.Y., Feng, S.B., et al., 2025. Innovative soaking-enhanced carbonated water flooding for EOR and CO_2 storage. Geoenergy Sci. Eng. 252, 213922. https://doi.org/10.1016/j.geoen.2025.213922.
Deng, J.L., 1989. Introduction to grey system theory. J. Grey Syst. 1 (1), 1–24. https://doi.org/10.1007/978-3-642-16158-2_1.
Dong, M., Foraie, J., Huang, S., et al., 2005. Analysis of immiscible water-alternating-gas (WAG) injection using micromodel tests. J. Can. Petrol. Technol. 44 (2), 17–25. https://doi.org/10.2118/0502-01.
Di, Z.C., Wang, Y.X., Chang, C.G., et al., 2025. Synergistic gas–slag scheme to mitigate CO_2 emissions from the steel industry. Nat. Sustain. 8, 763–772. https://doi.org/10.1038/s41893-025-01572-2.
Du, K.X., Wang, Z.J., Li, S.Y., et al., 2026. Improving fracture-matrix recovery in low-permeability reservoirs: an experimental study of huff-n-puff imbibition using active carbonated water. SPE J. 31 (2026), 572–587. https://doi.org/10.2118/231406-PA.
Esene, C., Rezaei, N., Aborig, A., et al., 2019. Comprehensive review of carbonated water injection for enhanced oil recovery. Fuel 237, 1086–1107. https://doi.org/10.1016/j.fuel.2018.08.106.
Foroozesh, J., Jamiolahmady, M., 2016. Simulation of carbonated water injection coreflood experiments: an insight into the wettability effect. Fuel 184, 581–589. https://doi.org/10.1016/j.fuel.2016.07.051.
Foroozesh, J., Jamiolahmady, M., 2018. The physics of CO_2 transfer during carbonated water injection into oil reservoirs: from non-equilibrium core-scale physics to field-scale implication. J. Petrol. Sci. Eng. 166, 798–805. https://doi.org/10.1016/j.petrol.2018.03.089.
Gan, X.W., Chen, Z.J., Ma, W.H., et al., 2025. Kinetic and thermodynamic analyses of multigranular low-rank coal: synergistic effect of particle size on reactivity and coke properties. Fuel 406, 137065. https://doi.org/10.1016/j.fuel.2025.137065.
Han, X.B., Yu, H.Y., Song, J.B., et al., 2025a. Enhanced oil recovery of tight oil reservoirs by active carbonated water imbibition: underlying mechanisms and influential factors. Phys. Fluids 37 (8), 086635. https://doi.org/10.1063/5.0280119.
Han, X.B., Yu, H.Y., Tang, H.T., et al., 2024. Investigation on oil recovery and countercurrent imbibition distance coupling carbonated water with surfactant in shale oil reservoirs. Fuel 374, 132409. https://doi.org/10.1016/j.fuel.2024.132409.
Han, X.B., Yu, H.Y., Wu, Y.H., et al., 2025b. Experimental investigation on the countercurrent imbibition distance and factors influencing the imbibition recovery of carbonated fracturing fluid. SPE J. 30 (3), 1474–1491. https://doi.org/10.2118/218205-PA.
Hao, Y.M., Li, Z.F., Su, Y.L., et al., 2022. Experimental investigation of CO_2 storage and oil production of different CO_2 injection methods at pore-scale and core-scale. Energy 254, 124349. https://doi.org/10.1016/j.energy.2022.124349.
Jeffry, L., Ong, M.Y., Nomanbhay, S., et al., 2021. Greenhouse gases utilization: a review. Fuel 301, 121017. https://doi.org/10.1016/j.fuel.2021.121017.
Kasala, E.E., Wang, J.J., Majid, A., et al., 2025. Enhancing CO_2 hydrate formation, stability and storage potential in sub-seafloor saline sediments using nanoparticle-assisted surfactant/polymer formulations: exploring molecular interaction to field application. Gas Sci. Eng. 134, 205544. https://doi.org/10.1016/j.jgsce.2025.205544.
Lin, Q.Y., Zhang, X., Wang, T., et al., 2022. Technical perspective of carbon capture, utilization, and storage. Engineering 14, 27–32. https://doi.org/10.1016/j.eng.2021.12.013.
Li, S.P., Yao, Z.Y., Shang, F.H., et al., 2025a. Improving CO_2 storage efficiency in saline aquifers through wettability-optimized nanoparticle foam. Phys. Fluids 37, 013351. https://doi.org/10.1063/5.0251254.
Li, Z.P., 2026. Toward low-carbon construction: a review of red mud utilization in cementitious materials and geopolymers for sustainability and cost benefits. Buildings 16 (2), 362. https://doi.org/10.3390/buildings16020362.
Li, S.P., Li, S.Y., Ma, R., 2025b. High-dryness foam for enhancing CO_2 storage efficiency in heterogeneous depleted reservoirs. Chem. Eng. J. 519, 165424. https://doi.org/10.1016/j.cej.2025.165424.
Liu, J.R., Zhang, D.F., Liu, S.Y., et al., 2025. Multiscale investigation into EOR mechanisms and influencing factors for CO_2-WAG injection in heterogeneous sandy conglomerate reservoirs using NMR technology. Pet. Sci. 22 (7), 2977–2991. https://doi.org/10.1016/j.petsci.2025.04.004.
Luo, X.J., Wei, B., Gao, K., et al., 2023. Gas channeling control with an in-situ smart surfactant gel during water-alternating-CO_2 enhanced oil recovery. Pet. Sci. 20 (5), 2835–2851. https://doi.org/10.1016/j.petsci.2023.03.003.
Majidaie, S., Khanifar, A., Onur, M., et al., 2012. A simulation study of chemically enhanced water alternating gas CWAG injection. In: Proceedings of SPE EOR Conference at Oil and Gas West Asia. https://doi.org/10.2118/154152-MS.
Nowrouzi, I., Manshad, A.K., Mohammadi, A.H., 2020. The mutual effects of injected fluid and rock during imbibition in the process of low and high salinity carbonated water injection into carbonate oil reservoirs. J. Mol. Liq. 305, 112432. https://doi.org/10.1016/j.molliq.2019.112432.
Pan, Y., Liu, H.Q., Tang, J., et al., 2024. Experimental study on carbonated water flooding enhanced volatile reservoirs recovery based on NMR technology. In: Proceedings of ADIPEC. https://doi.org/10.2118/222824-MS.
Qian, K., Yang, S.L., Dou, H.E., et al., 2019. Interaction of the CO_2-oil system and displacement mechanisms during CO_2 flooding. Pet. Sci. Bull. 4 (1), 69–82. https://doi.org/10.3969/j.issn.2096-1693.2019.01.006 (in Chinese).
Rahimi, A., Safari, M., Honarvar, B., et al., 2020. On time dependency of interfacial tension through low salinity carbonated water injection. Fuel 280, 118492. https://doi.org/10.1016/j.fuel.2020.118492.
Salehpour, M., Riazi, M., Malayeri, M.R., et al., 2020. CO_2-saturated brine injection into heavy oil carbonate reservoirs: investigation of enhanced oil recovery and carbon storage. J. Petrol. Sci. Eng. 195, 107663. https://doi.org/10.1016/j.petrol.2020.107663.
Seyyedi, M., Sohrabi, M., 2016. Enhancing water imbibition rate and oil recovery by carbonated water in carbonate and sandstone rocks. Energy Fuels. 30 (1), 285–293. https://doi.org/10.1021/acs.energyfuels.5b02644.
Seyyedi, M., Sohrabi, M., Farzaneh, A., 2015. Investigation of rock wettability alteration by carbonated water through contact angle measurements. Energy Fuels. 29 (9), 5544–5553. https://doi.org/10.1021/acs.energyfuels.5b01069.
Seyyedi, M., Sohrabi, M., Sisson, A., 2017. Experimental investigation of the coupling impacts of new gaseous phase formation and wettability alteration on improved oil recovery by CWI. J. Petrol. Sci. Eng. 150, 99–107. https://doi.org/10.1016/j.petrol.2016.11.016.
Shimokawara, M., Yogarajah, E., Nawa, T., et al., 2017. Carbon dioxide saturated water injection for EOR in carbonate reservoir. In: Proceedings of Abu Dhabi International Petroleum Exhibition & Conference. https://doi.org/10.2118/188936-MS.
Sohrabi, M., Emadi, A., Farzaneh, S.A., et al., 2015. A thorough investigation of mechanisms of enhanced oil recovery by carbonated water injection. In: Proceedings of SPE Annual Technical Conference and Exhibition. https://doi.org/10.2118/175159-MS.
Sohrabi, M., Kechut, N.I., Riazi, M., et al., 2011. Safe storage of CO_2 together with improved oil recovery by CO_2-enriched water injection. Chem. Eng. Res. Des. 89 (9), 1865–1872. https://doi.org/10.1016/j.cherd.2011.01.027.
Sohrabi, M., Riazi, M., Jamiolahmady, M., et al., 2009. Mechanisms of oil recovery by carbonated water injection. In: International Symposium of The society of Core Analysts. SCA2009-26.
Song, J.B., Yu, H.Y., Han, X.B., et al., 2025. Oil displacement and CO_2 storage mechanisms of impure CO_2 flooding in tight reservoirs: insights from microfluidic experiments and numerical simulations. Fuel 393, 134934. https://doi.org/10.1016/j.fuel.2025.134934.
Sun, Y.H., Wang, C., Qu, H.M., et al., 2024. Research progress of zwitterionic surfactants in the field of enhanced oil recovery in low-permeability reservoirs. Contemp. Chem. Ind. 53 (12), 2931–2935. https://doi.org/10.13840/j.cnki.cn21-1457/tq.2024.12.081.
Talebi, A., Hasan-Zadeh, A., Kazemzadeh, Y., et al., 2022. A review on the application of carbonated water injection for EOR purposes: opportunities and challenges. J. Petrol. Sci. Eng. 214, 110481. https://doi.org/10.1016/j.petrol.2022.110481.
Tan, X.H., Ma, X.J., Li, X.P., et al., 2025. An adsorption model considering fictitious stress. Fractal Fractional 9 (1), 17. https://doi.org/10.3390/fractalfract9010017.
Tang, M.R., Wang, C.W., Deng, X.A., et al., 2022. Experimental investigation on plugging performance of nanospheres in low-permeability reservoir with bottom water. Adv. Geo-Energy Res. 6 (2), 95–103. https://doi.org/10.46690/ager.2022.02.02.
Wang, S.S., Chen, C.L., Li, K.R., et al., 2019. In situ CO_2 enhanced oil recovery: parameters affecting reaction kinetics and recovery performance. Energy Fuels. 33, 3844–3854. https://doi.org/10.1021/acs.energyfuels.8b03734.
Wang, S.Y., Luo, F.Z., Wo, J.C., et al., 2025. Two-stage spatiotemporal decoupling configuration of SOP and multi-level electric-hydrogen hybrid energy storage based on feature extraction for distribution networks with ultra-high DG penetration. Appl. Energy 398, 126438. https://doi.org/10.1016/j.apenergy.2025.126438.
Wang, Z.J., Li, S.Y., Jin, Z.J., et al., 2023. Oil and gas pathway to net-zero: review and outlook. Energy Strategy Rev. 45, 101048. https://doi.org/10.1016/j.esr.2022.101048.
Wu, H.R., Chen, X., Tan, R., et al., 2022. Controllable regulation of emulsion stability by a pH-responsive zwitterionic/anionic surfactant system. Fuel 312, 122921. https://doi.org/10.1016/j.fuel.2021.122921.
Xie, C.Y., Wang, Y.J., Long, W.Q., et al., 2026. Numerical optimization of injection strategy for methanol engine with glow plug hot surface ignition system. Fuel 407, 137575. https://doi.org/10.1016/j.fuel.2025.137575.
Xiong, W., Zhao, Y.L., Zhang, L.H., et al., 2025. Mechanism study of enhanced gas recovery and CO_2 storage in naturally fractured carbonate reservoirs using a dual-permeability model coupled with association equation of state. Gas Sci. Eng. 139, 205632. https://doi.org/10.1016/j.jgsce.2025.205632.

Xu, L.P., Di, W., Liu, H.B., et al., 2025. Super-high bed homogeneous sintering for iron ores with low carbon emissions. J. Clean. Prod. 529, 146848. https://doi.org/10.1016/j.jclepro.2025.146848.

Xue, L., Zhang, J., Chen, G., et al., 2025. Enhance oil recovery by carbonized water flooding in tight oil reservoirs. Geoenergy Sci. Eng. 244, 213430. https://doi.org/10.1016/j.geoen.2024.213430.

Yuan, N., Wang, S.S., Yu, Y., et al., 2023. Expanded salinity window of middle-phase microemulsions and reduced surfactant adsorption by hydrotrope. Langmuir 39 (48), 17175–17189. https://doi.org/10.1021/acs.langmuir.3c02211.

Yu, H.Y., Rui, Z.H., Chen, Z.W., et al., 2019a. Feasibility study of improved unconventional reservoir performance with carbonated water and surfactant. Energy 182, 135–147. https://doi.org/10.1016/j.energy.2019.06.024.

Yu, H.Y., Yang, Z.L., Liu, J.H., et al., 2019b. EOR method by the carbonated water injection (CWI) for tight oil reservoirs. Pet. Geol. Oilfield Dev. Daqing 38 (2), 166–174. https://doi.org/10.19597/J.ISSN.1000-3754.201807019.

Zhang, L., Song, W., Huang, F., et al., 2026. Hydrate stability assessment in marine environments: Implications for CO_2 sequestration site optimization. Journal of Environmental Chemical Engineering 14 (2), 121641. https://doi.org/10.1016/j.jece.2026.121641.

Zhang, X., Wei, B., You, J.Y., et al., 2021. Characterizing pore-level oil mobilization processes in unconventional reservoirs assisted by state-of-the-art nuclear magnetic resonance technique. Energy 236, 121549. https://doi.org/10.1016/j.energy.2021.121549.

Zou, J.D., Liao, X.W., Chen, Z.M., et al., 2019. Integrated PVT and coreflooding studies of carbonated water injection in tight oil reservoirs: a case study. Energy Fuels. 33 (9), 8852–8863. https://doi.org/10.1021/acs.energyfuels.9b01243.

Zou, J.D., Liao, X.W., Li, X.M., et al., 2018. An experimental study on carbonated water injection of core samples from tight oil reservoirs from Ordos basin. In: Proceedings of SPE Russian Petroleum Technology Conference. https://doi.org/10.2118/191474-18RPTC-MS.